Remotely sensed land surface temperature is a proxy of ecosystem respiration in intact and disturbed northern peatlands

Iuliia Burdun[1], Ain Kull[1], Martin Maddison[1], Gert Veber[1], Oleksandr Karasov[1], Valentina Sagris[1], and Ülo Mander[1]

[1]Institute of Ecology & Earth Sciences, Department of Geography, University of Tartu, 46 Vanemuise St., Tartu 51014, Estonia

Corresponding author: Iuliia Burdun (iuliia.burdun@ut.ee)

Key Points:

- Temperature is a stronger driver of CO_2 fluxes in disturbed peatlands than in intact ones
- Remotely sensed land surface temperature is a strong predictor of in-situ thermal conditions in disturbed peatlands
- Ecosystem respiration can be modelled with remotely sensed land surface temperature in disturbed and intact northern peatlands

Abstract

Remotely sensed land surface temperature (LST) enables global modelling and monitoring carbon dioxide (CO_2) fluxes from peatlands. We aimed to provide the first overview of the LST potential for monitoring ecosystem respiration (R_{eco}) in disturbed (drained and extracted) peatlands. We used chamber measured data (2017–2020) from five disturbed and two intact northern peatlands and LST data from Landsat 7, 8, and MODIS missions. First, we studied the strength of relationships between fluxes and their in-situ drivers: thermal and moisture conditions. Second, we examined the association between LST and in-situ temperatures. Third, we compared chamber measured R_{eco} with the modelled R_{eco} based on (i) in-situ measured surface temperature and (ii) MODIS LST. In-situ temperatures were a stronger driver of CO_2 fluxes in disturbed sites (Spearman correlation R=0.8–0.9) than in intact ones (R=0.5–0.7). LST had a higher association with in-situ measured temperatures (mean R=0.74 for MODIS) in disturbed sites and weaker in the intact peatlands (mean R=0.34 for Landsat and 0.36 for MODIS). R_{eco} models driven by MODIS LST and in-situ surface temperature yielded similar accuracy: R^2 was 0.26, 0.64, 0.65 and 0.28, 0.68, 0.58 for intact, drained and extracted sites, correspondingly. Therefore, LST has a great potential to be utilized in R_{eco} models as a proxy of thermal regime in disturbed and intact northern peatlands.

Plain Language Summary

Organic carbon (C) in peat layer of peatlands has been accumulating for thousands of years. Under anthropogenic impact, e.g. drainage for forestry, agriculture or peat extraction, peatlands start emitting the accumulated C as carbon dioxide (CO_2) and methane (CH_4) back to the atmosphere much faster than historical rates of C accumulation. CO_2 and CH_4 are potent greenhouse gases that lead to climate warming. The thermal regime is among the main factors controlling CO_2 and CH_4 fluxes in peatlands. We demonstrated the potential of satellite thermal data for monitoring CO_2 fluxes from intact and disturbed peatlands. We used a long-term (2017–2020) dataset of CO_2 data measured in seven Estonian peatlands. The thermal regime explains CO_2 fluxes. Also, satellite thermal data better represent both the thermal regime and CO_2 fluxes in disturbed rather than in intact peatlands. Further, we modelled CO_2 fluxed from natural and disturbed peatlands: first, with thermal data measured in the field and, second, with satellite thermal data. Both these models resulted in similar prediction accuracy, which suggests that satellite thermal data have a great potential to be used for modelling CO_2 fluxes from peatlands of a varying range of disturbance.

1 Introduction

Peatlands cover only ~3% of the global land area (J. Xu, Morris, Liu, & Holden, 2018), though they store 21% of global terrestrial soil carbon (C) (Scharlemann, Tanner, Hiederer, & Kapos, 2014), which is double C in the world's forests (Pan et al., 2011). Approximately 80% of this peatland C stock is stored in northern peatlands – those distributed to the north of 45° N (Yu, Loisel, Brosseau, Beilman, & Hunt, 2010). Until now, intact northern peatlands act as a vast C sink and the average rate of C accumulation is estimated at 18.6 gC/m^2 per year (Yu, 2011).

Intact peatlands bound atmospheric carbon dioxide (CO_2) as C and accumulate it as peat (J.-O. Salm et al., 2012). However, at the same time, peatlands lose C with methane (CH_4)

emissions due to shallow (ground-) water table depths (WTD) and anoxic conditions in peat layer (Waddington & Roulet, 2000). CH_4 has more significant radiative efficiency than CO_2 but a much shorter lifetime in the atmosphere (Change, 2013). Therefore, over the millennial time scale, intact peatlands have a cooling effect on the Earth climate even though they are a source of CH_4 (Günther et al., 2020).

Over the last centuries, human impact and climate warming caused the lowering of WTD in peatlands, which led to oxidation of peat layer (Leifeld, Wüst-Galley, & Page, 2019; Regan, Flynn, Gill, Naughton, & Johnston, 2019; Swindles et al., 2019). Under warmer oxic conditions, peat layer decomposes and releases accumulated C as carbon dioxide (CO_2) (Hanson et al., 2020; Rinne et al., 2020; J. O. Salm, Kimmel, Uri, & Mander, 2009; Waddington, Rotenberg, & Warren, 2001). This loss of C can be 4.5 to 18 times faster than historical rates of C accumulation (Hanson et al., 2020). Hence, disturbed peatlands are a significant source of CO_2 and have a long-term climate warming impact (Leifeld et al., 2019; Ojanen, Minkkinen, & Penttilä, 2013). Particularly because of the CO_2 emissions from disturbed peatlands, the global peatland biome is expected to shift from sink to source already in this century (Leifeld et al., 2019; Loisel et al., 2021).

CO_2 exchange, particularly ecosystem respiration (R_{eco}), strongly depends on climatic conditions in disturbed peatlands, including soil and air temperatures (Maljanen et al., 2010; Veber et al., 2018). For example, a temperature-dependent function is widely used to model spatial and temporal R_{eco} from intact and disturbed peatlands (Alm et al., 2007; Bubier, Bhatia, Moore, Roulet, & Lafleur, 2003; Järveoja, Nilsson, Crill, & Peichl, 2020; Lafleur, Roulet, & Admiral, 2001). In previous studies, C fluxes were shown to have positive exponential relationships with peat temperatures at different depth: -20 cm (Helbig, Humphreys, & Todd, 2019), -10 cm (Davidson, Strack, Bourbonniere, & Waddington, 2019) and -5 cm (Acosta et al., 2017), as well as with surface temperature (X. Huang et al., 2021). However, the limited spatial coverage of in-situ temperature measurements enables the modelling of C fluxes only at the plot scale. Instead, the application of remotely sensed parameters, including land surface temperature (LST), can force the global modelling of R_{eco} in peatlands (Lees, Quaife, Artz, Khomik, & Clark, 2018).

Rahman et al. (2005) were one of the first who applied remotely sensed data for R_{eco} modelling. They found that MODIS LST had exponential relationships with R_{eco} over the wide range of North American land covers, and what is more, these relationships varied between land covers. Later, Kimball et al. (2009) developed a terrestrial carbon flux model driven by remotely sensed inputs for boreal biomes; however, none of the validation sites was located in peatland. After that, remotely sensed data were actively used to model C fluxes mainly for forest land covers (Crabbe, Janouš, Dařenová, & Pavelka, 2019; N. Huang, Gu, Black, Wang, & Niu, 2015; N. Huang, Gu, & Niu, 2014; Jägermeyr et al., 2014; Tang et al., 2011; Wu et al., 2014; Xiao et al., 2010). The major part of these studies utilized MODIS data of coarse spatial resolution (1-km for LST, 250 and 500-m for vegetation indices) together with C data measured at eddy towers and by chambers. So far, we know only two studies utilized remotely sensed data of higher spatial resolution – 30-m (Landsat) – for CO_2 fluxes estimation: the first one conducted over beech forest (Crabbe et al., 2019) and the second one – over forested peatland (C. Xu, Qu, Hao, Zhu, & Gutenberg, 2020).

Much less attention was paid to study relationships between R_{eco} and remotely sensed LST in peatlands. Schubert et al. (2010) revealed strong relationships between MODIS LST and

R_{eco} in different types of peatlands: bog (precipitation-fed) and fen (additionally fed with groundwater and, sometimes, surface runoff). Following, Gao et al. (2015) and Ai et al. (2018) developed models for R_{eco} simulation driven by MODIS LST and enhanced vegetation index (EVI). Those models were validated over large areas and diverse land covers, including marshes and wetlands. Generally, both these studies supported the idea of the strong relationship between R_{eco} and LST. More recently, Park et al. (2020) and Junttila et al. (2021) applied MODIS LST to estimate R_{eco} in tropical and northern peatlands, correspondingly. The case study on northern peatlands was limited only to five peatlands (four fens and one bog), even though it has demonstrated that the performance of LST varies between peatland types (Junttila et al., 2021).

Despite all the progress made in the estimation of R_{eco} with remotely sensed data, much uncertainty still remains about the strength of relationships between R_{eco} and LST in disturbed (drained and extracted) peatlands. To our knowledge, there is no study that has specifically addressed the applicability of LST for modelling CO_2 fluxes in those peatlands. We present the first attempt to cover this gap of knowledge to tap into the potential of remotely sensed LST – especially given the urgent need to manage substantial CO_2 emissions from disturbed peatlands. This article aims to quantitively assess relationships between R_{eco} and remotely sensed LST in drained, extracted and intact northern peatlands. We evaluated the applicability of LST for R_{eco} modelling in comparison to in-situ measured surface temperature. Overall, we used R_{eco} data from seven Estonian peatlands: in five of them, the peat extraction activity and water drainage were conducted in the past; two other peatlands are natural bog sites. Flux data were measured with closed chambers during the vegetation period in 2017–2020. We studied relationships between R_{eco} and LST data from MODIS Terra, Landsat 7 and Landsat 8 satellites. Finally, we examined the applicability of MODIS LST for R_{eco} modelling and compared the performance of this model with the model that utilizes in-situ measured surface temperature.

2 Materials and Methods

2.1 Study area

We collected R_{eco} data in seven boreal peatlands (Figure 1) with different types of management (Table 1) located in Estonia. In addition to CO_2 data, we measured CH_4 fluxes. The studied area has a temperate climate with long-term (1991–2020) mean annual temperature and precipitation of 7 ^{0}C and 662 mm, respectively (Estonian Weather Service, 2021). Figure 1 shows the location of studied peatlands (upper panel) and zoomed-in orthophotos of each peatland (bottom panels).

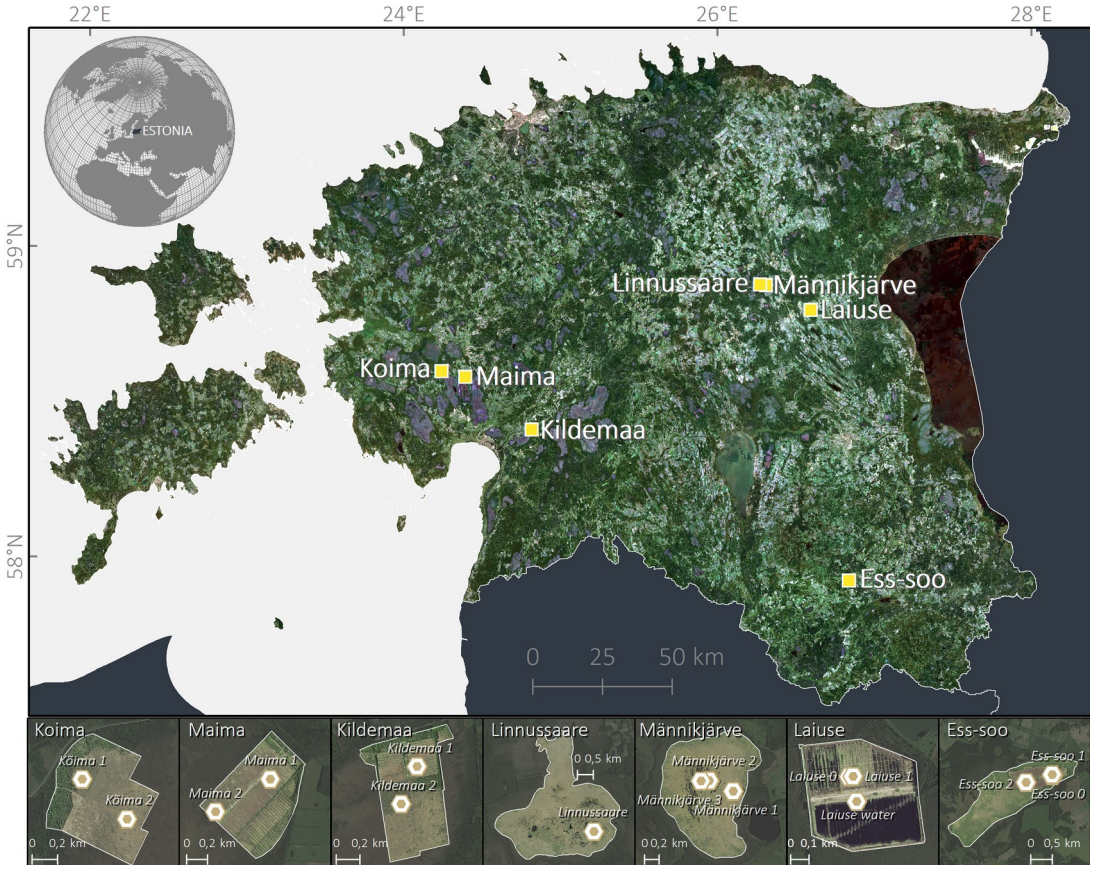

Figure 1. The study area includes seven boreal peatlands located in Estonia. The upper panel shows a true-coloured cloudless mosaic of Landsat 8 obtained for summer 2018. Bottom panels show locations of sites where ecosystem respiration was measured. Orthophotos for summertime in 2019 and 2020 are presented in the lower small panels (Estonian Land Board, 2020).

Ess-soo bog in southwest-Estonia is of limnogenic origin, and its peat layer varies from 4 to 6 meters, and in abandoned (in 1994) milled peat extraction site – from 2 to 4 meters. Vegetation cover in abandoned milled peat extraction area is sparse, dominated by *Eriophorum vaginatum, Calluna vulgaris, Empetrum nigrum, Vaccinium uliginosum, Polytrichum strictum, Betula pubescens and Pinus sylvestris*.

Kildemaa study site in the northern part of Kõrsa bog comprises abandoned milled peat production site (remaining peat layer depth 0.8–2 meters) and densely drained part of the bog prepared for peat extraction but abandoned before extraction (peat deposit up to 3 meters). Extracted site is sparsely vegetated with *Eriophorum vaginatum, Calluna vulgaris, Rhynchospora alba, Betula pubescens and Pinus sylvestris*, while the drained part is densely covered with dwarf pines (*Pinus sylvestris*), *Calluna vulgaris, Ledum palustre,* lichens and mosses.

Kõima and Maima peatlands belong to the Lavassaare bog complex, where peat deposit depth reaches up to 7.5 meters. Kõima study site covers former peat extraction site and adjacent nearly pristine reference site in the northwest of Kõima bog. Peat was extracted by cutting the peat in peat blocks with a machine or by hand. The extraction site was abandoned in the 1980s

and left for natural recovery. Ditches and depressions are mainly recovered with *Sphagnum* species, and drained unexcavated parts are covered with *Calluna vulgaris, Ledum palustre, Rubus chamaemorus, Andromeda polifolia and Pinus sylvestris*. In Maima, milled peat extraction took place until the 1990s. After abandonment, the site is only sparsely vegetated with *Eriophorum vaginatum, Calluna vulgaris, Oxycoccus palustris, Vaccinium uliginosum, Betula pubescens and Pinus sylvestris*.

Laiuse bog is of limnogenic origin and situated between drumlins. Mining activity was ceased there in 1996, and the peatland was left for natural regeneration. The northern part was partly covered with *Polytrichum strictum, Eriophorum vaginatum, Calluna vulgaris, Betula pubescens, and Pinus sylvestris,* while the southern part was flooded due to beaver activity since 2013.

Linnussaare and Männikjärve bogs belong to the Endla Nature Reserve and are added to the Ramsar List of Wetlands of International Importance (no. 907). These peatlands are of limnogenic origin; their peat layer varies from 4 to 7 meters and consists of residual of Sphagnum, Bryales and Carex, and Pinus (Sillasoo et al., 2007). Vegetation includes dwarf pines (*Pinus sylvestris*), grasses and dwarf shrubs (*Calluna vulgaris, Eriophorum vaginatum, Chamaedaphne calyculata, Andromeda polifolia, Rhynchospora alba, Ledum palustre, Oxycoccus microcarpus, and Oxycoccus palustris*), and a wide variety of *Sphagnum* mosses (*Sphagnum fuscum, Sphagnum balticum, Sphagnum magellanicum, and Sphagnum rubellum*) (Burdun, Bechtold, Sagris, Komisarenko, et al., 2020).

Table 1

Overview of peatland sites

Sampling position	Land management	Number of chambers (ch.) and microtopographic units	Dominant species	Lat.	Lon.
			Ess-soo		
Ess-soo 0	mined	4 ch.	*Eriophorum vaginatum, Calluna vulgaris, Vaccinium uliginosum, Polytrichum strictum, Betula pubescens and Pinus sylvestris*	57.914	26.697
Ess-soo 1	mined	3 ch.	*Eriophorum vaginatum, Calluna vulgaris, Vaccinium uliginosum, Polytrichum strictum, Betula pubescens and Pinus sylvestris*	57.914	26.697
Ess-soo 2	mined	3 ch.	*Oxycoccus palustris, Empetrum nigrum, Vaccinium uliginosum, Polytrichum strictum, Eriophorum vaginatum, Calluna vulgaris*	57.913	26.687
			Kildemaa		
Kildemaa 1	mined	3 ch.	*Eriophorum vaginatum, Calluna vulgaris, Rhynchospora alba, Betula pubescens and Pinus sylvestris*	58.427	24.786
Kildemaa 2	drained	3 ch.	*Calluna vulgaris, Ledum palustre, Polytrichum strictum, Andromeda polifolia and Pinus sylvestris*	58.424	24.784
			Kõima		
Kõima 1	drained	3 ch.	Various *Sphagnum* species, *Calluna vulgaris, Ledum palustre, Rubus*	58.617	24.233

			chamaemorus, Andromeda polifolia and Pinus sylvestris		
Kõima 2	natural	3 ch. at lawn	Various *Sphagnum* species, *Calluna vulgaris, Andromeda polifolia and Pinus sylvestris*	58.614	24.239
			Laiuse		
Laiuse 0	mined	4 ch.	*Polytrichum strictum, Eriophorum vaginatum, Calluna vulgaris, Betula pubescens and Pinus sylvestris*	58.790	26.528
Laiuse1	mined	3 ch.	*Polytrichum strictum, Eriophorum vaginatum, Calluna vulgaris and Pinus sylvestris*	58.790	26.528
Laiuse water	mined	1 floating ch.		58.789	26.529
			Linnussaare		
Linnussaare	natural	3 ch. at hollows, 3 ch. at hummocks, 1 floating ch. in pool	Various *Sphagnum* species, *Ledum palustre, Vaccinium uliginosum, Calluna vulgaris and Pinus sylvestris*	58.878	26.219
			Maima		
Maima 1	mined	3 ch.	*Eriophorum vaginatum, Calluna vulgaris, Oxycoccus palustris, Vaccinium uliginosum, Betula pubescens and Pinus sylvestris*	58.599	24.379
Maima 2	mined	3 ch.	*Eriophorum vaginatum, Rhynchospora alba, Calluna vulgaris and Pinus sylvestris*	58.596	24.370
			Männikjärve		
Männikjärve 1	natural	2 ch. at hollows, 2 ch. at hummocks	*Various Sphagnum species, Calluna vulgaris, Chamaedaphne calyculata, Rhynchospora alba, Ledum palustre, Oxycoccus microcarpus, Pinus sylvestris*	58.874	26.254
Männikjärve 2	natural	2 ch. at hollows, 2 ch. at hummocks	*Various Sphagnum species, Calluna vulgaris, Oxycoccus microcarpus, Carex*, *Pinus sylvestris*	58.876	26.249
Männikjärve 3	natural	2 floating ch.in pool, 2 ch. at hummocks	*Various Sphagnum species, Calluna vulgaris, Oxycoccus microcarpus, Pinus sylvestris*	58.876	26.247

2.2 Field-measurements of CO_2, CH_4, water table depth and soil temperature

We measured R_{eco} (CO_2) together with CH_4 fluxes with the closed-chamber method (Hutchinson & Livingston, 1993) during the vegetation period (March – November) in 2017–2020. Chambers (40 cm height, 50 cm diameter and 65 L volume) were made of polyvinyl chloride (PVC) and painted white to minimize their heating. The chambers were sealed with water-filled PVC collars (20 cm depth) on the peat surface. Each sampling site had replicants (Table 1) and was instrumented with piezometers (perforated pipes with 5 cm diameter and up to 1.5 m length). We sampled gas using pre-evacuated (0.3 mbar) glass vials (50 mL volume) every 20 minutes during a one-hour session. Later, gas concentration in vials was measured with Shimadzu GC-2014 gas-chromatography system equipped with an electron capture detector and a flame ionization detector. WTD was measured in piezometers on the same days when gas samples were collected. In addition to that, we measured soil temperature at the depths -10 cm (T_{10}), -20 cm (T_{20}), -30 cm (T_{30}) and -40 cm (T_{40}), and surface soil temperature (T_0).

193 2.3 Flux calculation

194 Fluxes of CO_2 and CH_4 were calculated from the linear change in gas concentration in a
195 chamber over 20 minutes time intervals. We adjusted gas concentration by the surface area
196 enclosed by collar and chamber volume. After that, we filtered out samples with a determination
197 coefficient (R^2) of the linear fit < 0.95 (p-value < 0.01) and fluxes changes below the gas-
198 chromatographer accuracy (20 ppm for CO_2 and 20 ppb for CH_4). Additionally, we filtered out
199 CH_4 values higher than 30000 µg C m^{-2} h^{-1} interpreted as ebullition fluxes. For the final analyses,
200 we calculated CO_2 and CH_4 fluxes as average across replicates in each sampling position (Table
201 1). The fluxes data were grouped by peatlands' management type and microtopographic
202 characteristics. As a result, we obtained five groups: flooded sites (data from floating chambers
203 in Männikjärve 3, Linnussaare and Laiuse water), hollows (Männikjärve 1, Männikjärve 2 and
204 Linnussaare), hummocks (Männikjärve 1 – Männikjärve 3, Linnussaare and Kõima 2), drained
205 sites (Kõima 1 and Kildemaa 2) and extracted sites (Ess-soo 0 – Ess-soo 2, Kildemaa 1, Laiuse 0,
206 Laiuse 1, Maima 1 and Maima 2). Figure 2 shows the changes in CO_2 and CH_4 fluxes in 2017–
207 2020 for those five groups.

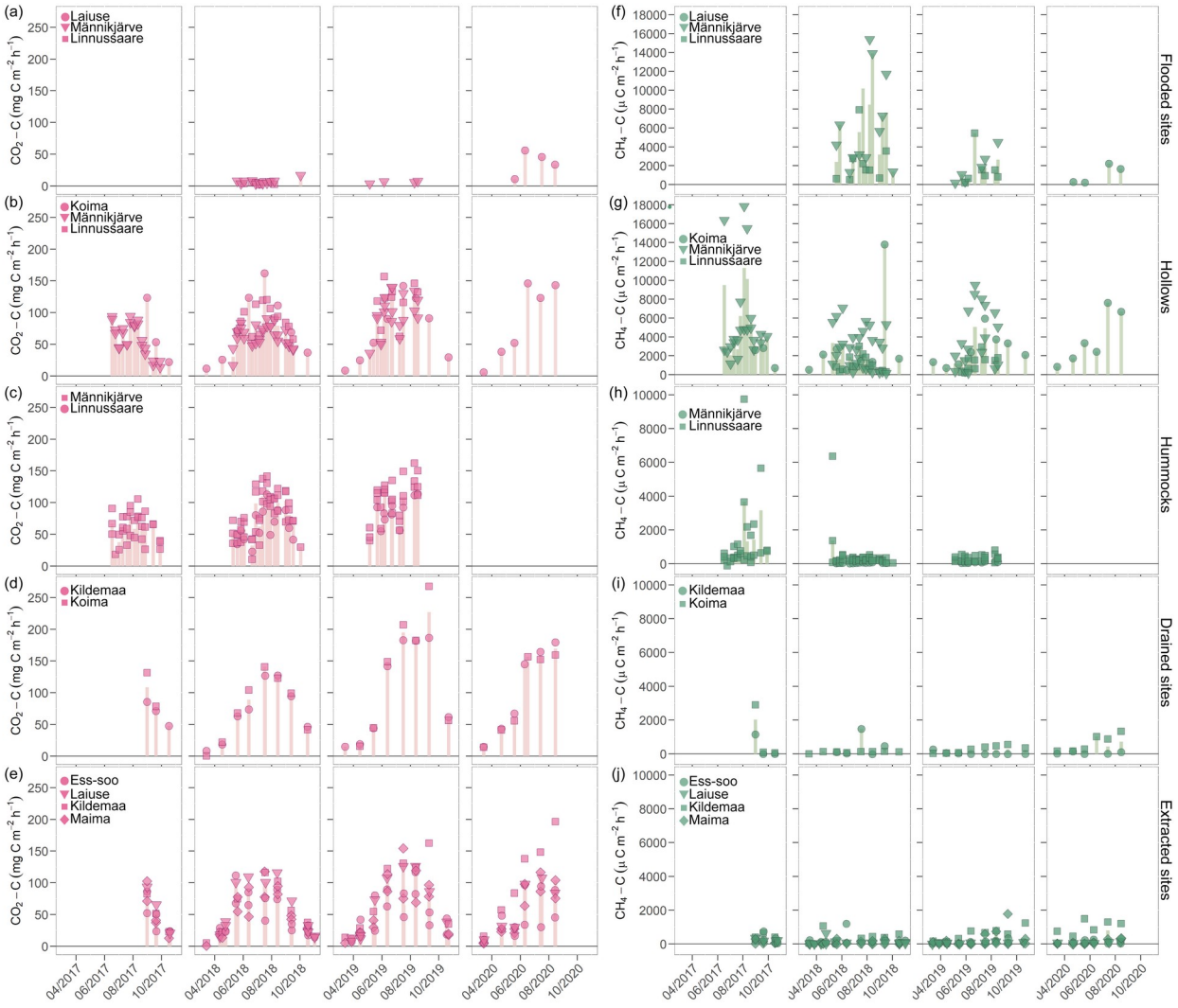

208

209 **Figure 2**. Time-series of CO_2 and CH_4 fluxes: one-time measured values (marks) and
210 averaged for each day (bars) for flooded sites (a, f), hollows (b, g), hummocks (c, h), drained (d,
211 i), and extracted sites (e, j).

212 2.4. Landsat and MODIS LST

213 We calculated LST from Landsat 7 and Landsat 8 data in Google Earth Engine (GEE)
214 online platform using open-source code by Ermida et al. (2020). This LST retrieval algorithm
215 utilizes Landsat thermal infrared and optical (to derive the Normalized Difference Vegetation
216 Index – NDVI) data, total column water vapour values from NCEP/NCAR reanalysis data, and
217 ASTER GEDv3 dataset to estimate surface emissivity. All these datasets are freely available in
218 GEE (Gorelick et al., 2017).

219 The field sampling campaign was carried out in the days when Landsat 7 or Landsat 8
220 overpassed the study area. Because of cloudy weather conditions, we had to mask out a lot of
221 LST pixels around the sampling sites. Thus, we decided to calculate the median Landsat LST
222 value over each peatland for each time scene (Figure 3). This decision increases data availability
223 for analyses, but, at the same time, it brings uncertainty since Landsat LST values can vary up to
224 6 ^{0}C within one peatland (Figure S1).

225 MODIS abroad Terra provides MOD11A1 daily LST product of 1 km spatial resolution
226 (Wan Z., Hook S., 2015). We masked pixels covered with clouds and shadows using the quality
227 control band, which is included in MOD11A1 dataset in GEE. Similar to Landsat LST data, we
228 calculated MODIS LST value as a median across all the pixels that cover peatland for each time
229 scene. MODIS LST values were well-agreed with Landsat LST values (Figure S2). Nevertheless,
230 the slope of relationships between MODIS LST and Landsat LST varies from 0.778 to 0.887 for
231 different peatlands, which means that under warmer conditions, there are higher Landsat LST
232 values in comparison to MODIS LST values, and under cooler conditions vice-verse: lower
233 Landsat LST values in comparison to MODIS LST values. The final number of Landsat and
234 MODIS images correspondingly is the following: 167 and 420 for Ess-soo, 88 and 387 for
235 Kildemaa, 131 and 387 for Kõima, 78 and 302 for Laiuse, 111 and 441 for Linnussaare, 95 and
236 379 for Maima, 98 and 372 for Männikjärve (Figure 3).

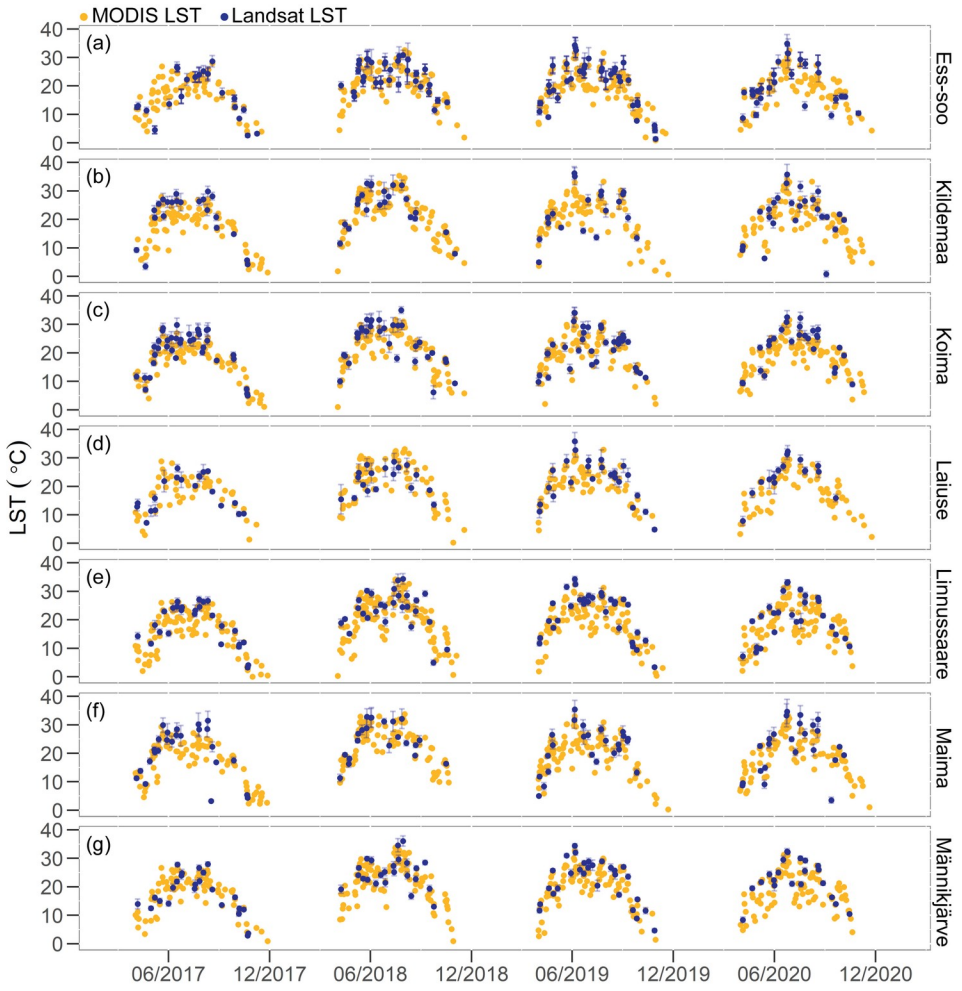

Figure 3. Time-series of MODIS LST median (yellow circles), Landsat LST median values (blue circles) and Landsat LST standard deviation within peatlands area (blue error bars).

2.5 R_{eco} modelling

We modelled R_{eco} following the approach presented by Tuittila et al. (2004). We utilized model adjusted by Gaussian curve functions of a second term that account for additional WTD and phenological phase effects (Eq. 1) as in (Järveoja et al., 2016; Riutta, Laine, & Tuittila, 2007):

$$R_{eco} = R_{ref}\, e^{E_0\left(\frac{1}{T_{ref}-T_0}-\frac{1}{T-T_0}\right)} \times e^{-0.5\times\left(\frac{Pp-Pp_{opt}}{Pp_{tol}}\right)^2} \times e^{-0.5\times\left(\frac{WTD-WTD_{opt}}{WTD_{tol}}\right)^2}, \quad (1)$$

where R_{ref} (mg CO_2 m^{-2} h^{-1}) is the respiration rate at 10 ^{0}C, E_0 (K) denotes temperature sensitivity, T_{ref} (^{0}C) is a reference temperature set at 10 ^{0}C, T_0 (^{0}C) is temperature minimum at which respiration reaches zero set at -46.021 ^{0}C, Pp (day) denotes the days in a phenological phase that starts in spring when the daily average air temperature is above 5 ^{0}C (Jaagus & Ahas, 2000), Pp_{opt} (day) denotes the optimal day for maximum R_{eco} from the beginning of vegetation period, Pp_{tol} (day) is a vegetation period tolerance for maximum R_{eco}, WTD_{opt} (cm) is an optimal soil water level for respiration and WTD_{tol} (cm) denotes the soil water level tolerance (deviation from the optimum at which R_{eco} is 61% of its maximum). Table 2 presents the parameters utilized

in Eq. 1 that were fitted with a Microsoft Excel Solver tool for calculation of ecosystem respiration CO_2-response curve (Lobo et al., 2013).

Table 2

Parameters for ecosystem respiration (R_{eco}) model in intact (hummocks and hollows merged), drained and extracted peatlands

Model parameter	Intact (hummock, hollow)	Drained	Extracted
E_0	147.7	122.7	153.5
R_{ref}	50.8	109.8	63.6
Pp_{opt}	99.3	119.5	97.1
Pp_{tol}	106.6	65.2	70.8
WTD_{opt}	-29.3	-25.6	-22.2
WTD_{tol}	98.5	64.8	44.7

2.6. Statistical analysis

We averaged the collar flux data for replicates in each site (Table 1) for further statistical analysis to avoid pseudoreplication. Further, we applied principal component analysis (PCA) to derive information about the relationships among all in-situ measured variables and cluster data depending on the relevance of different variables for four different studied groups, namely hummocks, hollows, drained and extracted sites. We did not include flooded sites to PCA since no WTD data were available for them. Before PCA analysis, the variables were standardized to zero mean. To evaluate the statistical dependency between paired variables, we applied a non-parametric Spearman rank correlation (R) with p-value < 0.05 statistical significance. The goodness of model performance was evaluated with R-squared (R^2) and root-mean-square error (RMSE) statistics. All statistics were computed using R software (R Core Team, 2018).

3 Results

3.1. Environmental controls on CO_2 and CH_4

In Figure 4, PCA of in-situ data shows the separation between different peatland groups. In-situ data projected onto the first two principal components (PC), explaining 78.4% of the variance in data. PC1 is positively correlated with temperature conditions and CO_2 fluxes, whereas PC2 is positively correlated with CH_4 fluxes and WTD. The distributions of intact (hummocks and hollows) and disturbed (drained and extracted) sites are well separated by high CH_4 fluxes and WTD. At the same time, the distributions of all four groups shows minor separation along PC1.

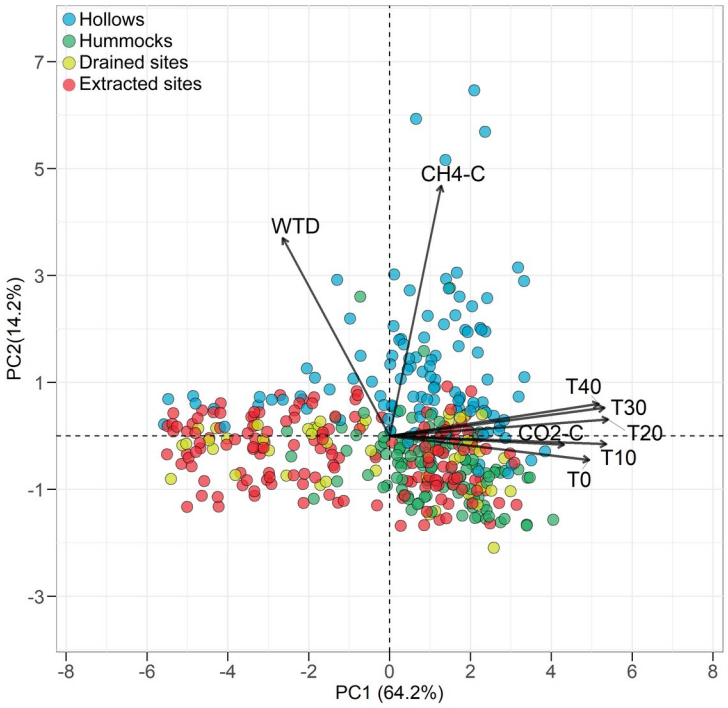

Figure 4. Principal component analysis for in-situ measured data for hollows (blue), hummocks (green), drained (yellow) and extracted (red) sites. PC1 and PC2 correspond to the first two principal components (PC).

To compare the relations between CO_2 and CH_4 fluxes and in-situ measured parameters, we performed Spearman correlation analysis. Figure 5 shows the correlation matrices for the studied peatland groups. The flooded sites stand out from others because their CO_2 and CH_4 fluxes do not have any statistically significant relations with in-situ parameters. Meanwhile, in other groups, CO_2 fluxes have from weak to strong R with temperatures and WTD. In hollows and hummocks, CO_2 fluxes have higher R values with surface and soil temperatures than with WTD. Both hollows and hummocks show higher R with CO_2 fluxes for upper soil layers. It is further noteworthy that R between CO_2 fluxes and $T_{0\text{-}40}$ in drained and extracted sites are higher than in intact sites. The highest R is observed between CO_2 fluxes and T_{20} in drained sites.

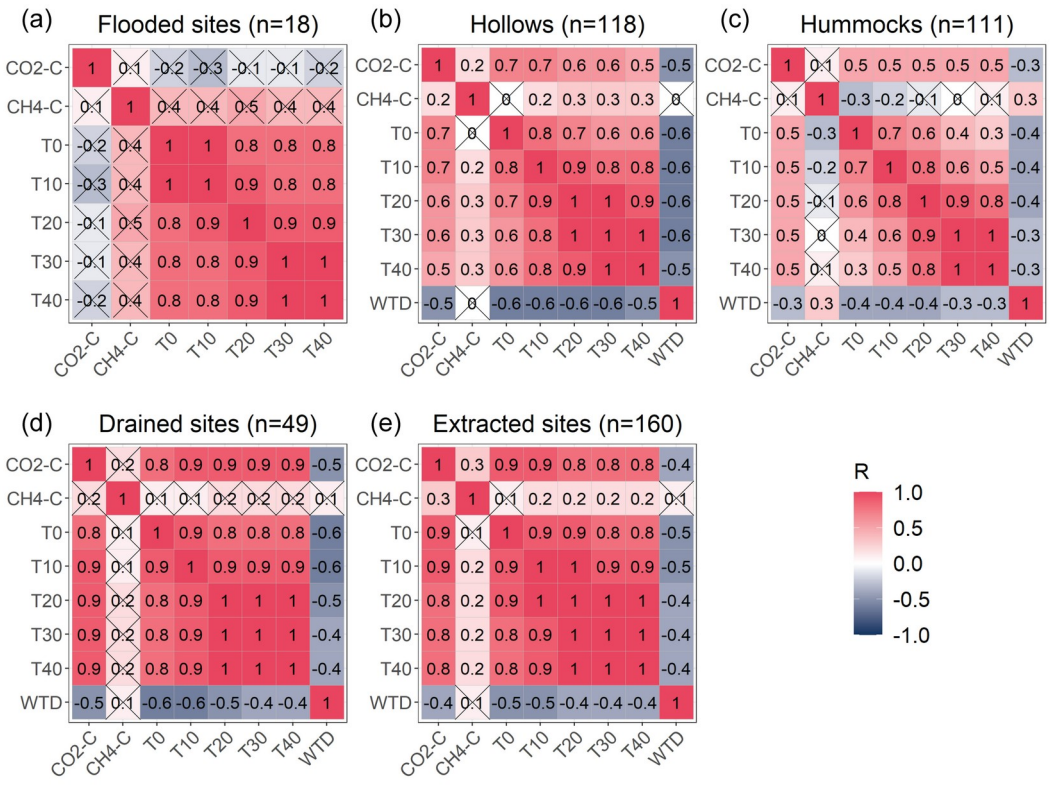

Figure 5. Spearman correlation (R) between CO_2 and CH_4 fluxes, water table depth (WTD), surface (T_0) and soil (T_{10}–T_{40}) temperatures. Intense red and blue colors indicate strong positive and negative R values, correspondingly. Crossed-out cells correspond to R values with p-value > 0.05.

Further, Figure 6 shows the relations between T_{10} and CO_2 and CH_4 fluxes for five studied groups. As it was previously shown in Figure 5, CO_2 fluxes are positively associated with temperature increase. Therefore, the maximum values of median CO_2 fluxes are observed in the summer months. In contrast, the lowest median values of CO_2 fluxes are present at the beginning of spring (March and April) and the end of autumn (October). Also, the weak negative association between CO_2 fluxes and WTD is noticeable in Figure 6 (panels b-e). The positive association between CH_4 fluxes and T_{10} can be seen for hollows, flooded, drained and extracted sites (Figure 6, panels f, g, i). Similar to CO_2, the highest median CH_4 fluxes occur in summer.

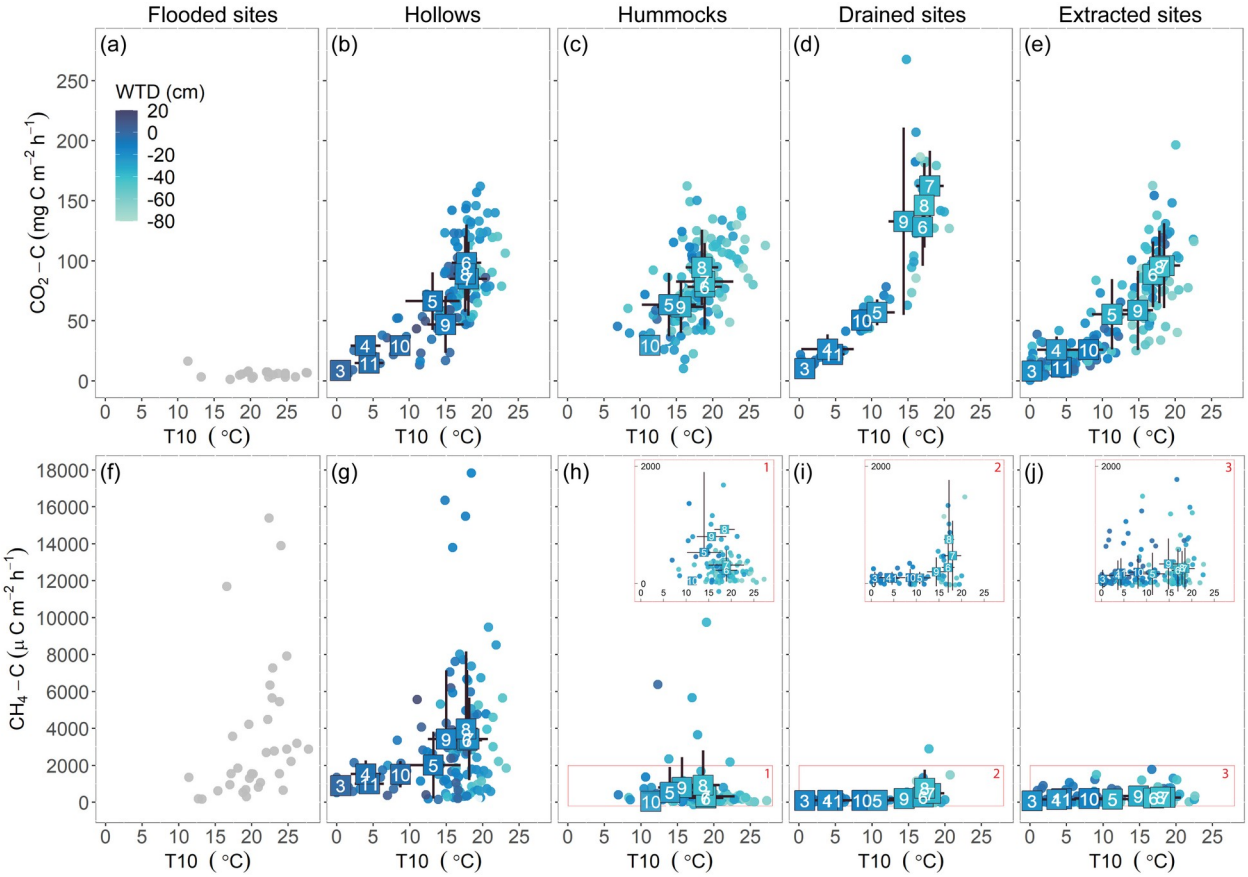

Figure 6. Scatterplots of soil temperature at a depth of 10 cm (T_{10}), CO_2 and CH_4 fluxes (circles). Monthly fluxes and T_{10} averages (square shapes with month numbers) are also given with monthly standard deviations (error bars). Colors indicate the water table depth (WTD) except for flooded sites, where no WTD data are available.

3.2. LST vs. in-situ temperatures

The profiles of temperature at different depths together with remotely-sensed Landsat and MODIS LST values are shown in Figure 7. We found that median peat temperatures generally decreased with depth; the highest temperature differential occurred between T_0 and T_{10}. Drained and extracted sites have wide peat temperature variability with bimodal distribution (Figure 7, panels d-e). In contrast, hummocks, hollows and flooded sites have lower temperature variability and close to normal temperature distribution almost at all the depths (Figure 7, panels a-c).

We further estimated R between LST and in-situ measured temperatures. For all the sites except flooded, both MODIS (Figure 7, panels b-e) and Landsat LST (Figure 7, panels b-c) had the highest R with T_0. Noteworthy that R between LST and in-situ temperatures were higher for disturbed sites than for intact ones. The magnitudes of the deviations between R values for MODIS LST and Landsat LST varied between 0.003–0.032 (Figure 7, panels b-c).

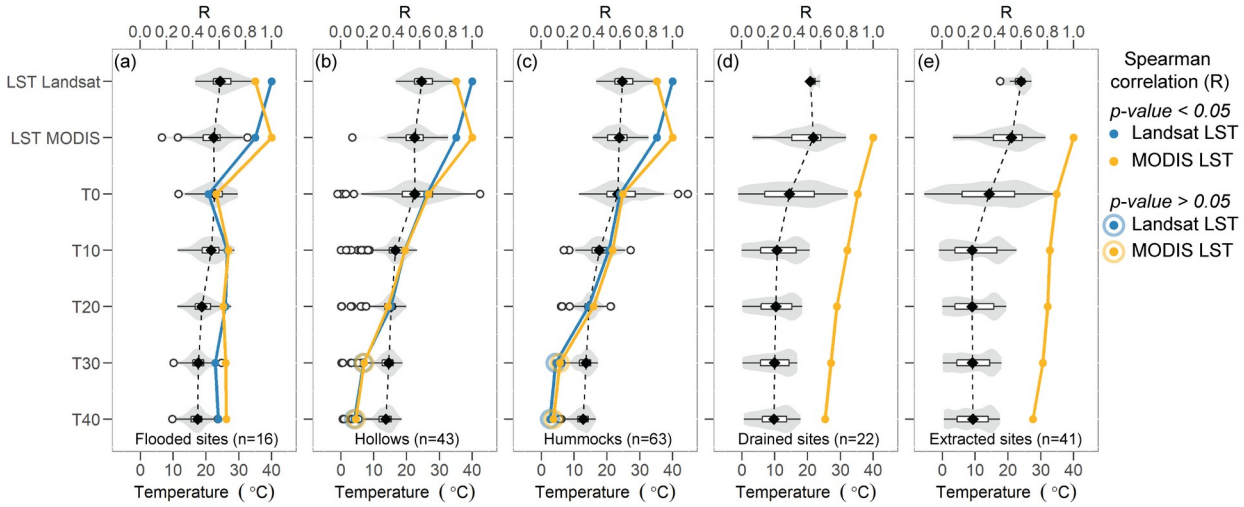

Figure 7. Profiles of temperature variation (boxplot) and distribution (shaded area) sensed by Landsat and MODIS, measured at the surface level (T_0) and 10–40 cm depths in the peat (T_{10}–T_{40}) for five studied groups. The median values (black diamond) for the mentioned temperatures are connected with a dashed line. Blue and orange dots represent Spearman correlation (R) between Landsat LST and MODIS LST correspondingly and in-situ measured temperatures.

3.3. Modelling R_{eco} with in-situ measured T_0 and remotely sensed MODIS LST

To estimate the potential of LST to be used instead of in-situ measured temperatures in R_{eco} modelling, we modelled CO_2 fluxes with T_0 as well as with MODIS LST data. We found that R_{eco} values were generally modelled with higher accuracy for disturbed peatlands (Figure 8). As shown in Figure 5, T_0 has a strong relationship with CO_2 fluxes in disturbed peatlands. Thus, R^2 values for the model, which utilized T_0, were 0.77 for the whole dataset and 0.68 for the days when MODIS LST data were available in drained sites. In extracted sites, those values were 0.64 and 0.58, correspondingly. Across the intact sites, R^2 values were notably lower: 0.38 and 0.28. When we further utilized MODIS LST instead of T_0 in the model (keeping other parameters the same) we found a similar pattern: R^2 higher for the disturbed sites (0.65 in extracted sites and 0.64 in drained sites) than for intact sites (0.26). Worth noticing that relatively high RMSE values were present in all the models.

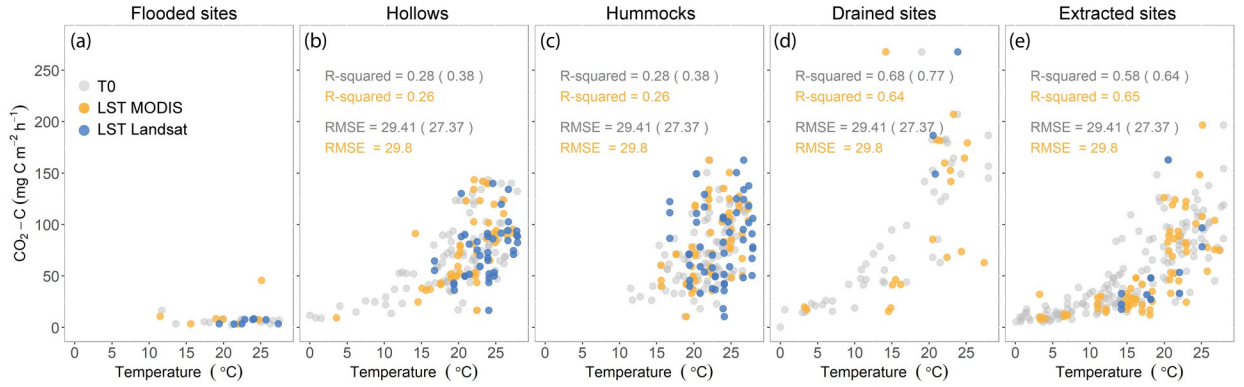

Figure 8. Scatterplots of CO_2 fluxes and MODIS LST (orange circle), Landsat LST (blue circle) and T_0 (grey circle) with modelled R^2 and RMSE (for the days when MODIS LST data were present and for the whole dataset – shown in round brackets) for five studied groups.

Comparison between measured and modelled CO_2 fluxes reveals that generally, we fail to catch the variability of CO_2 in intact sites (Figure 9 panel a). In particular, we observe the inability of the used modelling approach to model CO_2 fluxes higher than 100 mg C m^{-2} h^{-1} neither with T_0 nor with MODIS LST in the intact sites. Meanwhile, modelled CO_2 fluxes are better agreed with measured ones in disturbed sites (Figure 9 panels b, c). However, some obvious outliers are noticeable for the highest CO_2 fluxes, for which CO_2 fluxes were modelled with lower values. We found that those outliers were present in the model output forced with T_0 as well as with MODIS LST.

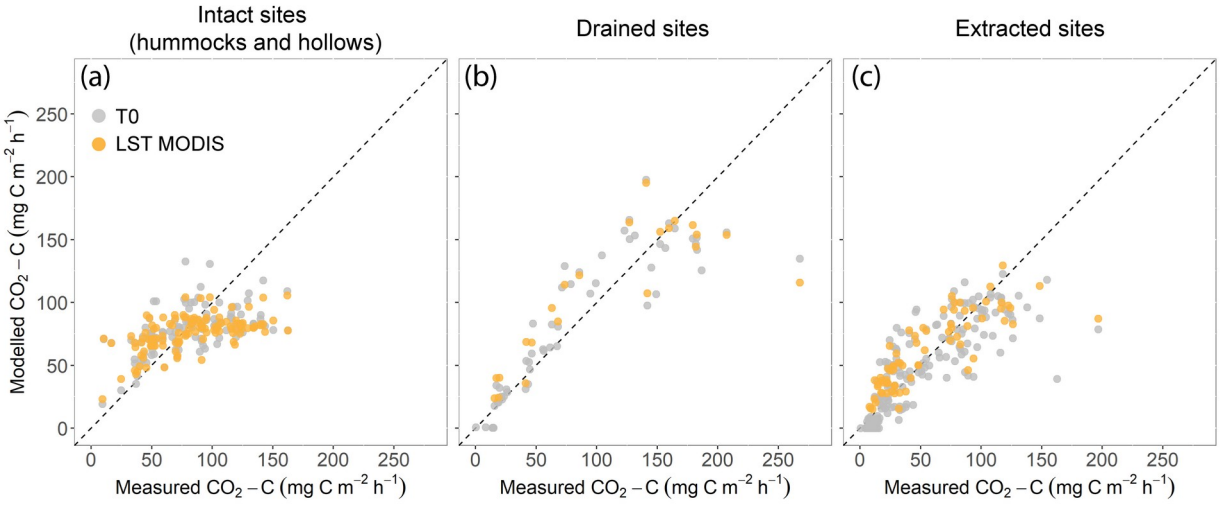

Figure 9. CO_2 fluxes measured in situ and modelled with surface temperature – T_0 (grey circle) – and remotely sensed MODIS LST (orange circle) for intact (joint hummocks and hollows), drained and extracted sites. The dashed line shows a 1:1 line.

4 Discussion

Prior studies have noted the importance of LST for R_{eco} estimations in different ecosystems. So far, none of the studies has addressed the potential of LST as a proxy of in-situ measured temperatures for modelling R_{eco} in disturbed peatlands. Here, we enriched the current knowledge and provided evidence for the future application of LST for that purpose. Even though we utilized daytime MODIS LST data of 1-km spatial resolution, we still managed to detect the temporal dynamics in in-situ measured temperatures at plot scale (Figure 7). This is particularly important for disturbed sites, where R_{eco} was mainly driven by thermal conditions (Figure 5).

Using the model parameterized for T_0, we utilized LST instead of T_0 and obtained R^2 equal to 0.26 for modelled R_{eco} in intact sites, 0.64 and 0.65 in drained and extracted sites correspondingly. To compare, in a previous study by Junttila et al. (2021) that jointly used remotely sensed LST and EVI data, the average R^2 was 0.56 among five peatlands. Noticeable that the lowest R^2 was obtained for bog site (0.23), while for fen sites, R^2 was dramatically higher varying from 0.51 to 0.85. We did not have fen sites in our dataset; however, the modelling results for bogs are in line with those published by Junttila et al. (2021). Notably, it

might be the case that the use of additional remotely sensed data, e.g. vegetation indices, can improve the R_{eco} model performance. For instance, Schubert et al. (2010) obtained high R^2 for both Swedish bog ($R^2 = 0.89$) and fen ($R^2 = 0.83$) by involving LST, NDVI and EVI data from MODIS. Ai et al. (2018) modelled R_{eco} utilizing LST and EVI for a big dataset with nine wetland biomes and obtained R^2=0.59.

Generally, we observed a weak R between LST and in-situ temperatures, and between in-situ temperatures and CO_2 and CH_4 fluxes in intact sites. As it was already shown for bogs (Burdun, Sagris, & Mander, 2019), LST has from weak to moderate association with soil temperatures, and the strength of this association decreases with soil depth. LST dynamics is highly dictated by incident solar radiation, while deeper soil temperatures react slowly with fewer fluctuations (R. Huang et al., 2020). Additionally, we assume that weak R between LST and T_{10}–T_{40} could be partially caused by a higher heat capacity of saturated peat in natural sites with shallow WTD (Zhao & Si, 2019). In previous work, Burdun et al. (2019) has demonstrated that LST had higher R with T_{10}–T_{40} during summers with abnormally high temperatures and, correspondingly, deeper WTD. LST also reveals weaker R with T_0 in intact sites. We believe it was primarily caused by vegetation cover properties. Studied bogs are covered with dense vegetation, primary Sphagnum mosses, which demonstrate high water loss by evapotranspiration that is near the potential rate of open water evaporation (Joon Kim & Verma, 1996). Through evapotranspiration, mosses cool the surface and perform as a thermal insulation layer (Blok et al., 2011). For these reasons, the disturbed sites with deeper WTD, covered with sporadic sedges and open peat surface, had higher R between LST and T_0–T_{40}.

In this work, R_{eco} model was forced by in-situ measurements, among them were WTD time series. However, only a small number of peatlands have in-situ historical observations, which limits the future applicability of the provided model. It is possible, therefore, to use remotely sensed proxies of WTD: e.g., radar data (Asmuß, Bechtold, & Tiemeyer, 2019; Tampuu, Praks, Uiboupin, & Kull, 2020) and Optical Trapezoid Model – OPTRAM (Burdun, Bechtold, Sagris, Lohila, et al., 2020). Further, given the well-established respiration dependency on LST in disturbed sites, future work could focus on the benefit of the combined contribution of the various remotely sensed data. For example, LAI, NDVI and EVI were shown to increase the R_{eco} model accuracy over various biomes, including peatlands (Ai et al., 2018; Y. Gao et al., 2015; Junttila et al., 2021). Moreover, the parameterization of models separately for each peatland could increase the model performance (Junttila et al., 2021).

In contrast to earlier findings (Evans et al., 2021; Feng et al., 2020), in all the sites, R between CH_4 fluxes and in-situ measured parameters was weak (from -0.3 to 0.3) and frequently not statistically significant (p-value > 0.05). The highest correlation (R=0.3) was observed between CH_4 fluxes and $T_{20–40}$ in hollows. Additionally, we observed a positive association (p-value > 0.05) between CH_4 fluxes and water temperature in flooded sites. In Figure 2, it is noticeable that CH_4 fluxes follow the seasonal dynamics in flooded sites (panel f). Summer 2018 was warmer than summer 2019, so methane fluxes increased dramatically during 2018 and were the greatest in midsummer. Similar results were discussed in (McEnroe, Roulet, Moore, & Garneau, 2009), where a weak positive (p-value < 0.001) R was found between air temperature and CH_4 fluxes.

Our findings may be somewhat limited by a small number of sites and methodological constraints. First, we tested LST applicability only in seven sites where R_{eco} data were measured with the closed-chamber technique. It is well-known that chamber measurements of R_{eco} might

not accurately represent the fluxes at the landscape scale (Schrier-Uijl et al., 2010). Second, we applied MODIS LST data of 1-km spatial resolution. MODIS pixels' footprint covered neighboring territories around the peatlands, which could cause a bias in the association between in-situ measured R_{eco} and LST. We did not utilize Landsat LST for R_{eco} modelling because of the very limited number of cloud-free images for the disturbed sites. This lack of data occurred even though we calculated one median Landsat LST value over one site for each time scene to increase the number of Landsat LST data. Unfortunately, high latitudes – where 80% of peatland C stock is located (Tanneberger et al., 2017) – are frequently covered by clouds. In this regard, modelling of R_{eco} with high-resolution Landsat data is challenging in northern peatlands. A good alternative to the original Landsat LST data could be modelled Landsat LST data derived with temporal adaptive reflectance fusion model, e.g. STARFM (F. Gao, Masek, Schwaller, & Hall, 2006). The fusion algorithms for Landsat and MODIS imagery have already shown promising results (Moreno-Martinez et al., 2020). Additionally, machine learning techniques could be used to fill the gaps in Landsat LST images (Buo, Sagris, & Jaagus, 2021).

Altogether, our results highlight that remotely sensed LST is a powerful tool for modelling R_{eco}. LST has the potential to be used in drained and extracted sites with deep WTD and covered with sparse sedges. However, more studies are needed to identify how general our findings are across disturbed peatlands in the Northern Hemisphere.

5 Conclusions

The purpose of this study was to estimate the strength of relationships between R_{eco} and LST and in disturbed (drained and extracted) and intact peatlands. Particularly, we aimed to examine the applicability of MODIS LST for R_{eco} modelling and compare the performance of the MODIS LST-driven model with the model driven by in-situ measured surface temperature. This study indicates that LST has a great potential to be utilized in R_{eco} models as a proxy of thermal conditions in northern peatlands. The highest R (mean 0.74) was observed between LST and in-situ measured T_0 –T_{40} for drained and extracted sites. However, at intact sites, the relationships between LST and T_0 –T_{40} were dramatically weaker: mean R over hummocks and hollows was 0.34 for Landsat and 0.36 for MODIS. R_{eco} model driven by MODIS LST yielded similar accuracy as the model driven by in-situ T_0: R^2 was 0.28, 0.68 and 0.58 for intact (hummocks and hollows), drained and extracted sites with T_0-driven model, and 0.26, 0.64 and 0.65 with MODIS LST-driven model.

The present study has been one of the first attempts to thoroughly examine the potential of remotely sensed LST for monitoring C fluxes at drained and extracted peatlands. Though our study was limited only to seven peatlands with intermitted R_{eco} time-series stemmed from manual closed-chamber technique, we showed that LST data could be used as a tool to monitor CO_2 fluxes with relatively high accuracy. Future research should be carried out to identify how general our findings are across disturbed peatlands in the Northern Hemisphere.

Acknowledgments, Samples, and Data

The authors are grateful to Dr Alar Teemusk for gas sample analyses at the laboratory of the Department of Geography, Institute of Ecology and Earth Sciences, University of Tartu, Estonia.

Field measured data reported in this study will be available at the zenodo.org repository. The authors will publish this dataset as soon as possible. For now, we attach this dataset as supplementary material.

This work was financially supported by the Estonian Research Council (research grats PRG-352 and MOBERC20), the European Commission through the European Regional Development Fund (the Center of Excellence EcolChange), the European Commission and ETAG for funding ERA-NET Cofund project WaterJPI-JC-2018_13: ReformWater and the Estonian State Forest Management Centre (project LLTOM17250 "Water level restoration in cut-away peatlands: development of integrated monitoring methods and monitoring", 2017–2023).

References

Acosta, M., Juszczak, R., Chojnicki, B., Pavelka, M., Havránková, K., Lesny, J., … Olejnik, J. (2017). CO2 Fluxes from Different Vegetation Communities on a Peatland Ecosystem. *Wetlands*, *37*(3), 423–435. https://doi.org/10.1007/s13157-017-0878-4

Agarwal, R., & Garg, J. K. (2009). Methane emission modelling from wetlands and waterlogged areas using MODIS data on JSTOR. *Current Science*, *96*(1), 36–40. Retrieved from https://www.jstor.org/stable/24104725?seq=1#metadata_info_tab_contents

Ai, J., Jia, G., Epstein, H. E., Wang, H., Zhang, A., & Hu, Y. (2018). MODIS-Based Estimates of Global Terrestrial Ecosystem Respiration. *Journal of Geophysical Research: Biogeosciences*, *123*(2), 326–352. https://doi.org/10.1002/2017JG004107

Alm, J., Shurpali, N. J., Minkkinen, K., Aro, L., Hytönen, J., Laurila, T., … Laine, J. (2007). Emission factors and their uncertainty for the exchange of CO2, CH4 and N2O in Finnish managed peatlands. *Boreal Environment Research*, *12*, 191–209. Retrieved from https://jukuri.luke.fi/handle/10024/513695

Asmuß, T., Bechtold, M., & Tiemeyer, B. (2019). On the Potential of Sentinel-1 for High Resolution Monitoring of Water Table Dynamics in Grasslands on Organic Soils. *Remote Sensing*, *11*(14), 1659. https://doi.org/10.3390/rs11141659

Blok, D., Heijmans, M., Schaepman-Strub, G., van Ruijven, J., Parmentier, F. J. W., Maximov, T. C., & Berendse, F. (2011). The Cooling Capacity of Mosses: Controls on Water and Energy Fluxes in a Siberian Tundra Site. *Ecosystems*, *14*(7), 1055–1065. https://doi.org/10.1007/s10021-011-9463-5

Bubier, J. L., Bhatia, G., Moore, T. R., Roulet, N. T., & Lafleur, P. M. (2003). *Spatial and Temporal Variability in Growing-Season Net Ecosystem Carbon Dioxide Exchange at a Large Peatland in Ontario, Canada*. https://doi.org/10.1007/s10021-003-0125-0

Buo, I., Sagris, V., & Jaagus, J. (2021). Gap-Filling Satellite Land Surface Temperature Over Heatwave Periods With Machine Learning. *IEEE Geoscience and Remote Sensing Letters*, 1–5. https://doi.org/10.1109/LGRS.2021.3068069

Burdun, I., Bechtold, M., Sagris, V., Komisarenko, V., De Lannoy, G., & Mander, Ü. (2020). A comparison of three trapezoid models using optical and thermal satellite imagery for water table depth monitoring in Estonian bogs. *Remote Sensing*, *12*(12), 1–24. https://doi.org/10.3390/rs12121980

Burdun, I., Bechtold, M., Sagris, V., Lohila, A., Humphreys, E., Desai, A., … Mander, Ü. (2020). Localizing pixels with SWIR-based moisture index representative of overall peatland water table dynamics. *Remote Sensing*.

Burdun, I., Sagris, V., & Mander, Ü. (2019). Relationships between field-measured hydrometeorological variables and satellite-based land surface temperature in a hemiboreal raised bog. *International Journal of Applied Earth Observation and Geoinformation*, *74*, 295–301. https://doi.org/10.1016/j.jag.2018.09.019

Change, I. P. on C. (2013). Anthropogenic and natural radiative forcing. In *Climate Change 2013 the Physical Science Basis: Working Group I Contribution to the Fifth Assessment Report of the Intergovernmental Panel on Climate Change* (Vol. 9781107057999, pp. 659–740). Cambridge University Press. https://doi.org/10.1017/CBO9781107415324.018

Crabbe, R. A., Janouš, D., Dařenová, E., & Pavelka, M. (2019). Exploring the potential of LANDSAT-8 for estimation of forest soil CO 2 efflux. *International Journal of Applied Earth Observation and Geoinformation*, *77*, 42–52. https://doi.org/10.1016/j.jag.2018.12.007

Davidson, S. J., Strack, M., Bourbonniere, R. A., & Waddington, J. M. (2019). Controls on soil carbon dioxide and methane fluxes from a peat swamp vary by hydrogeomorphic setting. *Ecohydrology*, *12*(8), e2162. https://doi.org/10.1002/eco.2162

Ermida, S. L., Soares, P., Mantas, V., Göttsche, F.-M., & Trigo, I. F. (2020). Google Earth Engine Open-Source Code for Land Surface Temperature Estimation from the Landsat Series. *Remote Sensing*, *12*(9), 1471. https://doi.org/10.3390/rs12091471

Estonian Land Board. (2020). Orthophotos. Retrieved July 2, 2020, from https://geoportaal.maaamet.ee/index.php?page_id=309&lang_id=2

Estonian Weather Service. (2021). Estonian Weather Service. Retrieved February 25, 2021, from https://www.ilmateenistus.ee/?lang=en

Evans, C. D., Peacock, M., Baird, A. J., Artz, R. R. E., Burden, A., Callaghan, N., … Morrison, R. (2021). Overriding water table control on managed peatland greenhouse gas emissions. *Nature*, 1–7. https://doi.org/10.1038/s41586-021-03523-1

Feng, X., Deventer, M. J., Lonchar, R., Ng, G. H. C., Sebestyen, S. D., Roman, D. T., … Kolka, R. K. (2020). Climate Sensitivity of Peatland Methane Emissions Mediated by Seasonal Hydrologic Dynamics. *Geophysical Research Letters*, *47*(17), e2020GL088875. https://doi.org/10.1029/2020GL088875

Gao, F., Masek, J., Schwaller, M., & Hall, F. (2006). On the blending of the landsat and MODIS surface reflectance: Predicting daily landsat surface reflectance. *IEEE Transactions on Geoscience and Remote Sensing*, *44*(8), 2207–2218. https://doi.org/10.1109/TGRS.2006.872081

Gao, Y., Yu, G., Li, S., Yan, H., Zhu, X., Wang, Q., … Zhang, J. (2015). A remote sensing model to estimate ecosystem respiration in Northern China and the Tibetan Plateau. *Ecological Modelling*, *304*, 34–43. https://doi.org/10.1016/j.ecolmodel.2015.03.001

Gorelick, N., Hancher, M., Dixon, M., Ilyushchenko, S., Thau, D., & Moore, R. (2017). Google Earth Engine: Planetary-scale geospatial analysis for everyone. *Remote Sensing of*

Environment, *202*, 18–27. https://doi.org/10.1016/j.rse.2017.06.031

Günther, A., Barthelmes, A., Huth, V., Joosten, H., Jurasinski, G., Koebsch, F., & Couwenberg, J. (2020). Prompt rewetting of drained peatlands reduces climate warming despite methane emissions. *Nature Communications*, *11*(1), 1–5. https://doi.org/10.1038/s41467-020-15499-z

Hanson, P. J., Griffiths, N. A., Iversen, C. M., Norby, R. J., Sebestyen, S. D., Phillips, J. R., … Ricciuto, D. M. (2020). Rapid Net Carbon Loss From a Whole−Ecosystem Warmed Peatland. *AGU Advances*, *1*(3), e2020AV000163. https://doi.org/10.1029/2020AV000163

Helbig, M., Humphreys, E. R., & Todd, A. (2019). Contrasting Temperature Sensitivity of CO2 Exchange in Peatlands of the Hudson Bay Lowlands, Canada. *Journal of Geophysical Research: Biogeosciences*, *124*(7), 2126–2143. https://doi.org/10.1029/2019JG005090

Huang, N., Gu, L., Black, T. A., Wang, L., & Niu, Z. (2015). Remote sensing-based estimation of annual soil respiration at two contrasting forest sites. *Journal of Geophysical Research: Biogeosciences*, *120*(11), 2306–2325. https://doi.org/10.1002/2015JG003060

Huang, N., Gu, L., & Niu, Z. (2014). Estimating soil respiration using spatial data products: A case study in a deciduous broadleaf forest in the Midwest USA. *Journal of Geophysical Research: Atmospheres*, *119*(11), 6393–6408. https://doi.org/10.1002/2013JD020515

Huang, R., Huang, J. X., Zhang, C., Ma, H. Y., Zhuo, W., Chen, Y. Y., … Mansaray, L. R. (2020). Soil temperature estimation at different depths, using remotely-sensed data. *Journal of Integrative Agriculture*, *19*(1), 277–290. https://doi.org/10.1016/S2095-3119(19)62657-2

Huang, X., Silvennoinen, H., Kløve, B., Regina, K., Kandel, T. P., Piayda, A., … Höglind, M. (2021). Modelling CO2 and CH4 emissions from drained peatlands with grass cultivation by the BASGRA-BGC model. *Science of the Total Environment*, *765*, 144385. https://doi.org/10.1016/j.scitotenv.2020.144385

Hutchinson, G. L., & Livingston, G. P. (1993). *Use of Chamber Systems to Measure Trace Gas Fluxes*. John Wiley & Sons, Ltd. https://doi.org/10.2134/asaspecpub55.c4

Jaagus, J., & Ahas, R. (2000). Space-time variations of climatic seasons and their correlation with the phenological development of nature in Estonia. *Climate Research*, *15*(3), 207–219. https://doi.org/10.3354/cr015207

Jägermeyr, J., Gerten, D., Lucht, W., Hostert, P., Migliavacca, M., & Nemani, R. (2014). A high-resolution approach to estimating ecosystem respiration at continental scales using operational satellite data. *Global Change Biology*, *20*(4), 1191–1210. https://doi.org/10.1111/gcb.12443

Järveoja, J., Nilsson, M. B., Crill, P. M., & Peichl, M. (2020). Bimodal diel pattern in peatland ecosystem respiration rebuts uniform temperature response. *Nature Communications*, *11*(1), 1–9. https://doi.org/10.1038/s41467-020-18027-1

Järveoja, J., Peichl, M., Maddison, M., Soosaar, K., Vellak, K., Karofeld, E., … Mander, Ü. (2016). Impact of water table level on annual carbon and greenhouse gas balances of a restored peat extraction area. *Biogeosciences*, *13*(9), 2637–2651. https://doi.org/10.5194/bg-13-2637-2016

Joon Kim, & Verma, S. B. (1996). Surface exchange of water vapour between an open

sphagnum fen and the atmosphere. *Boundary-Layer Meteorology*, *79*(3), 243–264. https://doi.org/10.1007/bf00119440

Junttila, S., Kelly, J., Kljun, N., Aurela, M., Klemedtsson, L., Lohila, A., … Eklundh, L. (2021). Upscaling Northern Peatland CO2 Fluxes Using Satellite Remote Sensing Data. *Remote Sensing*, *13*(4), 818. https://doi.org/10.3390/rs13040818

Kimball, J. S., Jones, L. A., Zhang, K., Heinsch, F. A., McDonald, K. C., & Oechel, W. C. (2009). A satellite approach to estimate land-atmosphere CO2 exchange for boreal and Arctic biomes using MODIS and AMSR-E. *IEEE Transactions on Geoscience and Remote Sensing*, *47*(2), 569–587. https://doi.org/10.1109/TGRS.2008.2003248

Lafleur, P. M., Roulet, N. T., & Admiral, S. W. (2001). Annual cycle of CO_2 exchange at a bog peatland. *Journal of Geophysical Research: Atmospheres*, *106*(D3), 3071–3081. https://doi.org/10.1029/2000JD900588

Lees, K. J., Quaife, T., Artz, R. R. E., Khomik, M., & Clark, J. M. (2018). Potential for using remote sensing to estimate carbon fluxes across northern peatlands – A review. *Science of the Total Environment*, Vol. 615. https://doi.org/10.1016/j.scitotenv.2017.09.103

Leifeld, J., Wüst-Galley, C., & Page, S. (2019, December 1). Intact and managed peatland soils as a source and sink of GHGs from 1850 to 2100. *Nature Climate Change*, Vol. 9, pp. 945–947. Nature Research. https://doi.org/10.1038/s41558-019-0615-5

Lobo, F. de A., de Barros, M. P., Dalmagro, H. J., Dalmolin, Â. C., Pereira, W. E., de Souza, É. C., … Rodríguez Ortíz, C. E. (2013). Fitting net photosynthetic light-response curves with Microsoft Excel - a critical look at the models. *Photosynthetica*, *51*(3), 445–456. https://doi.org/10.1007/s11099-013-0045-y

Loisel, J., Gallego-Sala, A. V., Amesbury, M. J., Magnan, G., Anshari, G., Beilman, D. W., … Wu, J. (2021). Expert assessment of future vulnerability of the global peatland carbon sink. *Nature Climate Change*, *11*(1), 70–77. https://doi.org/10.1038/s41558-020-00944-0

Maljanen, M., Sigurdsson, B. D., Guömundsson, J., Öskarsson, H., Huttunen, J. T., & Martikainen, P. J. (2010). Greenhouse gas balances of managed peatlands in the Nordic countries present knowledge and gaps. *Biogeosciences*, *7*(9), 2711–2738. https://doi.org/10.5194/bg-7-2711-2010

McEnroe, N. A., Roulet, N. T., Moore, T. R., & Garneau, M. (2009). Do pool surface area and depth control CO_2 and CH_4 fluxes from an ombrotrophic raised bog, James Bay, Canada? *Journal of Geophysical Research*, *114*(G1), G01001. https://doi.org/10.1029/2007JG000639

Moreno-Martinez, A., Izquierdo-Verdiguier, E., Camps-Valls, G., Moneta, M., Munoz-Mari, J., Robinson, N., … Running, S. W. (2020). Down-Scaling Modis Vegetation Products with Landsat GAP Filled Surface Reflectance in Google Earth Engine. *International Geoscience and Remote Sensing Symposium (IGARSS)*, 2320–2323. Institute of Electrical and Electronics Engineers Inc. https://doi.org/10.1109/IGARSS39084.2020.9324007

Ojanen, P., Minkkinen, K., & Penttilä, T. (2013). The current greenhouse gas impact of forestry-drained boreal peatlands. *Forest Ecology and Management*, *289*, 201–208. https://doi.org/10.1016/j.foreco.2012.10.008

622 Pan, Y., Birdsey, R. A., Fang, J., Houghton, R., Kauppi, P. E., Kurz, W. A., … Hayes, D. (2011).
623 A large and persistent carbon sink in the world's forests. *Science*, *333*(6045), 988–993.
624 https://doi.org/10.1126/science.1201609

625 Park, H., Takeuchi, W., & Ichii, K. (2020). Satellite-Based Estimation of Carbon Dioxide Budget
626 in Tropical Peatland Ecosystems. *Remote Sensing*, *12*(2), 250.
627 https://doi.org/10.3390/rs12020250

628 R Core Team. (2018). *R: A Language and Environment for Statistical Computing*. Vienna,
629 Austria: R Foundation for Statistical Computing. Retrieved from https://www.r-project.org/

630 Rahman, A. F., Sims, D. A., Cordova, V. D., & El-Masri, B. Z. (2005). Potential of MODIS EVI
631 and surface temperature for directly estimating per-pixel ecosystem C fluxes. *Geophysical*
632 *Research Letters*, *32*(19), n/a-n/a. https://doi.org/10.1029/2005GL024127

633 Regan, S., Flynn, R., Gill, L., Naughton, O., & Johnston, P. (2019). Impacts of Groundwater
634 Drainage on Peatland Subsidence and Its Ecological Implications on an Atlantic Raised
635 Bog. *Water Resources Research*, *55*(7), 6153–6168.
636 https://doi.org/10.1029/2019WR024937

637 Rinne, J., Tuovinen, J. P., Klemedtsson, L., Aurela, M., Holst, J., Lohila, A., … Nilsson, M. B.
638 (2020). Effect of the 2018 European drought on methane and carbon dioxide exchange of
639 northern mire ecosystems: 2018 drought on northern mires. *Philosophical Transactions of*
640 *the Royal Society B: Biological Sciences*, *375*(1810). https://doi.org/10.1098/rstb.2019.0517

641 Riutta, T., Laine, J., & Tuittila, E. S. (2007). Sensitivity of CO2 exchange of fen ecosystem
642 components to water level variation. *Ecosystems*, *10*(5), 718–733.
643 https://doi.org/10.1007/s10021-007-9046-7

644 Salm, J.-O., Maddison, M., Tammik, S., Soosaar, K., Truu, J., & Mander, Ü. (2012). Emissions
645 of CO2, CH4 and N2O from undisturbed, drained and mined peatlands in Estonia.
646 *Hydrobiologia*, *692*(1), 41–55. https://doi.org/10.1007/s10750-011-0934-7

647 Salm, J. O., Kimmel, K., Uri, V., & Mander, Ü. (2009). Global warming potential of drained and
648 undrained Peatlands in Estonia: A synthesis. *Wetlands*, *29*(4), 1081–1092.
649 https://doi.org/10.1672/08-206.1

650 Scharlemann, J. P. W., Tanner, E. V. J., Hiederer, R., & Kapos, V. (2014). Global soil carbon:
651 Understanding and managing the largest terrestrial carbon pool. *Carbon Management*, *5*(1),
652 81–91. https://doi.org/10.4155/cmt.13.77

653 Schrier-Uijl, A. P., Kroon, P. S., Hensen, A., Leffelaar, P. A., Berendse, F., & Veenendaal, E. M.
654 (2010). Comparison of chamber and eddy covariance-based CO2 and CH4 emission
655 estimates in a heterogeneous grass ecosystem on peat. *Agricultural and Forest*
656 *Meteorology*, *150*(6), 825–831. https://doi.org/10.1016/j.agrformet.2009.11.007

657 Schubert, P., Eklundh, L., Lund, M., & Nilsson, M. (2010). Estimating northern peatland CO2
658 exchange from MODIS time series data. *Remote Sensing of Environment*, *114*(6), 1178–
659 1189. https://doi.org/10.1016/j.rse.2010.01.005

660 Sillasoo, U., Mauquoy, D., Blundell, A., Charman, D., Blaauw, M., Daniell, J. R. G., …
661 Karofeld, E. (2007). Peat multi-proxy data from Männikjärve bog as indicators of late
662 Holocene climate changes in Estonia. *Boreas*, *36*(1), 20–37. https://doi.org/10.1111/j.1502-

3885.2007.tb01177.x

Swindles, G. T., Morris, P. J., Mullan, D. J., Payne, R. J., Roland, T. P., Amesbury, M. J., … Warner, B. (2019). Widespread drying of European peatlands in recent centuries. *Nature Geoscience*, *12*(11), 922–928. https://doi.org/10.1038/s41561-019-0462-z

Tampuu, T., Praks, J., Uiboupin, R., & Kull, A. (2020). Long Term Interferometric Temporal Coherence and DInSAR Phase in Northern Peatlands. *Remote Sensing*, *12*(10), 1566. https://doi.org/10.3390/rs12101566

Tang, X., Liu, D., Song, K., Munger, J. W., Zhang, B., & Wang, Z. (2011). A new model of net ecosystem carbon exchange for the deciduous-dominated forest by integrating modis and flux data. *Ecological Engineering*, *37*(10), 1567–1571. https://doi.org/10.1016/j.ecoleng.2011.03.030

Tanneberger, F., Tegetmeyer, C., Busse, S., Barthelmes, A., Shumka, S., Mariné, A. M., … Joosten, H. (2017). The peatland map of Europe. *Mires and Peat*, *19*. https://doi.org/10.19189/MaP.2016.OMB.264

Tuittila, E.-S., Vasander, H., & Laine, J. (2004). Sensitivity of C Sequestration in Reintroduced Sphagnum to Water-Level Variation in a Cutaway Peatland. *Restoration Ecology*, *12*(4), 483–493. https://doi.org/10.1111/j.1061-2971.2004.00280.x

Veber, G., Kull, A., Villa, J. A., Maddison, M., Paal, J., Oja, T., … Mander, Ü. (2018). Greenhouse gas emissions in natural and managed peatlands of America: Case studies along a latitudinal gradient. *Ecological Engineering*, *114*, 34–45. https://doi.org/10.1016/j.ecoleng.2017.06.068

Waddington, J. M., Rotenberg, P. A., & Warren, F. J. (2001). Peat CO2 production in a natural and cutover peatland: Implications for restoration. *Biogeochemistry*, *54*(2), 115–130. https://doi.org/10.1023/A:1010617207537

Waddington, J. M., & Roulet, N. T. (2000). Carbon balance of a boreal patterned peatland. *Global Change Biology*, *6*(1), 87–97. https://doi.org/10.1046/j.1365-2486.2000.00283.x

Wan Z., Hook S., H. G. (2015). *MOD11A1 MODIS/Terra Land Surface Temperature/Emissivity Daily L3 Global 1km SIN Grid V006*. NASA EOSDIS Land Processes DAAC. https://doi.org/https://doi.org/10.5067/MODIS/MOD11A1.006

Wu, C., Gaumont-Guay, D., Andrew Black, T., Jassal, R. S., Xu, S., Chen, J. M., & Gonsamo, A. (2014). Soil respiration mapped by exclusively use of MODIS data for forest landscapes of Saskatchewan, Canada. *ISPRS Journal of Photogrammetry and Remote Sensing*, *94*, 80–90. https://doi.org/10.1016/j.isprsjprs.2014.04.018

Xiao, J., Zhuang, Q., Law, B. E., Chen, J., Baldocchi, D. D., Cook, D. R., … Wofsy, S. C. (2010). A continuous measure of gross primary production for the conterminous United States derived from MODIS and AmeriFlux data. *Remote Sensing of Environment*, *114*(3), 576–591. https://doi.org/10.1016/j.rse.2009.10.013

Xu, C., Qu, J. J., Hao, X., Zhu, Z., & Gutenberg, L. (2020). Monitoring soil carbon flux with in-situ measurements and satellite observations in a forested region. *Geoderma*, *378*, 114617. https://doi.org/10.1016/j.geoderma.2020.114617

Xu, J., Morris, P. J., Liu, J., & Holden, J. (2018). PEATMAP: Refining estimates of global

704 peatland distribution based on a meta-analysis. *Catena*, *160*, 134–140.
705 https://doi.org/10.1016/j.catena.2017.09.010

706 Yu, Z. (2011). Holocene carbon flux histories of the world's peatlands. *The Holocene*, *21*(5),
707 761–774. https://doi.org/10.1177/0959683610386982

708 Yu, Z., Loisel, J., Brosseau, D. P., Beilman, D. W., & Hunt, S. J. (2010). Global peatland
709 dynamics since the Last Glacial Maximum. *Geophysical Research Letters*, *37*(13).
710 https://doi.org/10.1029/2010GL043584

711 Zhao, Y., & Si, B. (2019). Thermal properties of sandy and peat soils under unfrozen and frozen
712 conditions. *Soil and Tillage Research*, *189*, 64–72.
713 https://doi.org/10.1016/j.still.2018.12.026

714